Renewable Energy 154 (2020) 841–848

Contents lists available at ScienceDirect

Renewable Energy

journal homepage: www.elsevier.com/locate/renene

Flow sculpting enabled anaerobic digester for energy recovery from low-solid content waste

Sophia Ghanimeh [a, *], Charbel Abou Khalil [a], Daniel Stoecklein [c], Aditya Kommasojula [c], Baskar Ganapathysubramanian [c]

[a] Department of Civil and Environmental Engineering, Notre Dame University-Louaize, Lebanon
[c] Department of Mechanical Engineering, Iowa State University, USA

ARTICLE INFO

Article history:
Received 2 November 2019
Received in revised form
14 February 2020
Accepted 19 February 2020
Available online 22 February 2020

Keywords:
Anaerobic digester
Plug flow reactor
Low-solid-content wastewater
Food waste
Computational fluid dynamics

ABSTRACT

Traditionally, energy recovery from low-solid-content wastes occurs in Continuously Stirred Tank Reactors, whereas Plug Flow Reactors (PFR) are used to treat high-solid-content wastes. In comparison, this study uses a special configuration of anaerobic PFR (AnPFR), consisting of a coiled tubular structure, for energy recovery from a mixture of Food Waste and Wastewater, fed at a loading rate of 3 $gVS.L^{-1}.d^{-1}$ and a solids content of 2.5%. The AnPFR was upgraded into a Flow Sculpting enabled Anaerobic Digester (FSAD), an innovative plug flow design relying on flow sculpting via a sequence of pillars to provide passive mixing. The purpose of the FSAD design is to optimize operational performance while maintaining minimum mixing energy requirements. Computational fluid dynamics simulations revealed that pillars induce local vorticity in the fluid and contribute to the inertial deformation of the flow to enhance mixing. Coherently, experimental results proved that upgrading the AnPFR to FSAD resulted in a better stability (VFA dropped from 4433 to 2034 mg L^{-1}) and a higher efficiency (removal efficiencies of COD and volatile solids increased from 75% to 77%–88% and 91%, respectively). Equally important, the methane yield, indicative of energy generation potential, increased from 181 L kg VS_{fed}^{-1} to 291 L kg VS_{fed}^{-1}.

1. Introduction

Anaerobic digestion (AD) is a bioremediation method involving the biodegradation of organic matter by anaerobic microorganisms, leading to the formation of biogas (≈60% CH4; a renewable energy source) and treated effluent [1–3]. The most two common configurations are: Anaerobic Continuously Stirred Tank Reactor (AnCSTR) and Anaerobic Plug Flow Reactor (AnPFR), which are commonly used to treat wet and dry waste, respectively [4,5].

AD of waste with low-solid content (TS < 4%) often occurs in AnCSTR, with relatively long retention times, resulting in high cost-to-energy yield ratio [4,5]. For instance, AD of raw domestic wastewater (WW) is considered economically unfeasible because of high flow rate, requiring large anaerobic digester volumes, and low TS resulting in low CH_4 generation, poor performance, and low process efficiency [5–7]. Consequently, domestic WW is usually treated aerobically, using the activated sludge process, and only the residual sludge is collected and fed to an AnCSTR. The generated gas supplies a portion of the WWTP energy requirements [8]. However, most of the energy inherent in the carbonaceous material of the WW is lost through aerobic biochemical reactions, before reaching the AnCSTR [6].

Other bioreactor configurations and designs adopted in AD of low-solid WW include: Upflow Anaerobic Sludge Blanket (UASB) [9,10], Expanded Granular Sludge Blanket (EGSB) [11], and Anaerobic Membrane Bioreactor (AnMBR) [12,13], among others. UASB and the EGSB designs showed satisfactory (up to 80%) removal rates for both Chemical Oxygen Demand (COD) and Volatile Solids (VS) while generating up to 0.2 L CH4.g VSfed-1 [11,13–16]. Likewise, AnMBR applications achieved adequate (up to 90%) COD and VS removal rates [12,13,17]. However, AnMBR has high energy demand, compared to UASB and EGSB, with high risk of membrane fouling [12,13].

Abbreviations: AnPFR, Anaerobic Plug Flow Reactor; FSAD, Flow Sculpting enabled Anaerobic Digester; AnCSTR, Anaerobic Continuously Stirred Tank Reactor; AD, Anaerobic Digestion; UASB, Upflow Anaerobic Sludge Blanket; EGSB, Expanded Granular Sludge Bed; AnMBR, Anaerobic Membrane Bioreactor; WW, wastewater; FW, food waste; TS, total solids; TSS, total suspended solids; VS, volatile solids; VSS, volatile suspended solids; COD, chemical oxygen demand; VFA, volatile fatty acids; OLR, organic loading rate; HRT, hydraulic retention time; WWTP, wastewater treatment plant; CFD, Computational Fluid Dynamics.

* Corresponding author.
E-mail address: sghanimeh@ndu.edu.lb (S. Ghanimeh).

https://doi.org/10.1016/j.renene.2020.02.071
0960-1481/

In comparison, AnPFR is commonly used to treat high-solid-content waste (Total Solids (TS) > 10%), also known as high-strength waste, such as Food Waste (FW), organic fraction of municipal solid waste, agricultural waste, and sewage sludge, among others [5,18]. AnPFR showed several benefits, including low concentrations of VFA in the effluent, high degree of sludge retention, stable reactor performance, high conversion rates, low volume requirements, low initial investment cost, and simple operation and maintenance [5,19]. Yet, AnPFR is rarely used to treat low-solid-content wastes. Limited reported applications of wet AnPFR include the treatment of a mix of pineapple pulp and peel (TS < 4%) with an average COD removal of 70% and an average CH4 yield reaching 0.09 m^3/kg of CODremoved [20]. Also, inclined AnPFR was used to treat a mixture of kitchen waste at a TS of 7% [19], whereby VS and COD removal efficiencies reached 66–71% and 71–78%, respectively, at Hydraulic Retention Times (HRT) of 22.5 d and 33.7d. Likewise, high rate baffled AnPFR systems were used to treat low TS wastes (TS = 2.5%) at a low HRT of 24 h and reported a TS removal of 86% under mesophilic conditions [21]. However, studies on AD of low-solid waste using AnPFR with improved mixing are limited [5,6].

On the other hand, Stoecklein et al. [22] have recently demonstrated the ability to engineer the cross-sectional shape of a fluid using the integrated inertial flow deformations induced by sequences of pillars. The latter has proven to produce a rich phase space with a wide variety of flow transformations [22,23]. This concept has since been used to: (1) solve problems in biological and advanced manufacturing fields, (2) design polymer fiber cross-sections, (3) create 3-D particles, and (4) provide a solution to transfer around particles in flow, among others [22,23]. This is a promising, low-energy strategy to enhance mixing in digesters. However, this method has not been applied yet to PFR configurations or AD systems.

As to the feed mix, multiple studies addressed the co-digestion of different types of wastes to benefit from their complementary properties. Emphasis was put on adding FW to anaerobic digesters treating WW sludge, at TS ranging between 7 and 13%, to improve methane yield [24–26]. Due to its high-strength, FW possesses a high specific CH_4 yield varying from 200 to 500 L of CH_4 per $VS_{fed, wet}$ [5,27], which is triple the CH_4 generated from WW sludge [28]. However, considering the high biodegradability of FW, Volatile Fatty Acids (VFAs) generation occurs fast in the anaerobic digester, leading to pH drop and inhibition of methanogenic reactions [29,30]. As such, the presence of low-solid WW in the feed mix provides dilution of acids, and other inhibiting byproducts, resulting in improved process stability [5,29–31]. Yet, the concept of adding FW to raw WW, resulting in a feed of low TS content, hasn't been extensively tested.

In comparison with reported studies, this paper attempts to apply the AnPFR concept, through a coiled (multi layered) structure, for the treatment of low-strength (TS = 2.5%) waste, made of a mix of FW and WW. The coiled AnPFR design was upgraded into a Flow Sculpting enabled Anaerobic Digester (FSAD), a novel application of the flow sculpting approach, whereby cross-sectional deformations of the fluid are induced by sequences of pillars that disrupt the flow. This creates passive mixing and improves the net energy balance. To the best of the authors knowledge, no similar configuration has been reported for anaerobic digesters treating wastes. The key performance indicators were monitored, and conclusions were made as to the improvements associated with the FSAD design.

2. Methods

2.1. Experimental Setup

The lab-scale AnPFR (Fig. 1-a, Fig. 2) used in this experiment consists of 28.3 m of nylon tubing (3/8" inner diameter) with a total working volume of 2 L. The AnPFR (tubing) was coiled around a cylindrical Plexiglas structure (F) having a height of 1 m, diameter of 0.5 m, and a circumference of 1.6 m. The coiled assembly was placed inside a cubic chamber (H) constructed of Styrofoam with an inner volume of 3.4 m^3, in which two 250W infrared heater lamps were installed and connected to a temperature controller and a thermometer to maintain mesophilic conditions (37 ± 0.5 C). A fan was placed inside the chamber to improve air circulation and distribute the heat. For passive mixing, sets of eight conical pillars (base diameter = 5 mm (3/16") and height = 6.4 mm (1/4")) were inserted into the tubing (separated by 127 mm (5") along the centerline) and placed against the inner wall following, consecutively, the configuration shown in Fig. 1-b.

For feeding, a Plexiglas container (I) was connected to a peristaltic pump (G), which was in turn connected to the inlet of the AnPFR. The outlet was connected to an anaerobic tank (J) which has four openings: (J1) to receive the digestate, (J2) to withdraw the digestate, (J3) to recycle digestate into the digester, and (J4) to release the biogas into a wet tip gas meter (D). The latter is connected to a 10 L Tedlar bag (E) in order to capture the biogas generated and analyze its composition on a daily basis.

2.2. Waste preparation and feeding

The low-solid waste feed was prepared by mixing FW, prepared and shredded as in Ghanimeh et al. [30], with WW collected from an on-campus WWTP to achieve the required TS content of 2.5% (Table 1). The waste was stored in 0.5 L plastic bottles at −25 C. A semi-continuous feeding scheme was adopted, consisting of 30 min of continuous feeding every day, at a rate of 0.11 mL s^{-1}. A recirculation rate of 20% was adopted to increase the solid retention time and enhance anaerobic microbial abundance [32].

2.3. Start-up and operation

Inoculation was achieved by adding 2 L of digestate from a lab-scale operating mesophilic anaerobic digester treating FW. After a two-day incubation period, equal wasting and feeding was initiated. The system was loaded progressively, between weeks 1 and 5, until reaching an OLR of 3.0 g $VS.L^{-1}.d^{-1}$. During the entire experiment (30 weeks), the anaerobic digester was operated at an HRT of 14 days (2 weeks).

The experimental program consisted of two stages. In the first stage, the coiled tubular AnPFR was tested, with up-flow feeding and without induced mixing. After a five HRT start-up period, the digester was operated for another five HRT stabilization period (weeks 6–16), during which steady-state conditions were achieved. In the second stage, the AnPFR was upgraded by introducing the physical obstructions (pillars), as described in sub-section II.A, to induce passive mixing and test the novel FSAD design concept over a period equivalent to 7 HRTs (weeks 17–30).

2.4. Analytical methods

Physico-chemical parameters were monitored on a weekly basis (every Monday), including: TS, Total Suspended Solids (TSS), VS and Volatile Suspended Solids (VSS), using Standard Methods 2540B and 2540E procedures; COD by spectrophotometry, applying the modification of Standard Methods 5220D procedure [33] using HACH medium-range COD kits (HACH Company, Loveland, Colorado); ammonia concentration by spectrophotometry using HACH high range ammonia kits (HACH Company, Loveland, Colorado. The system stability was monitored by measuring total VFA levels weekly, by titration methods [34], and comparing them to

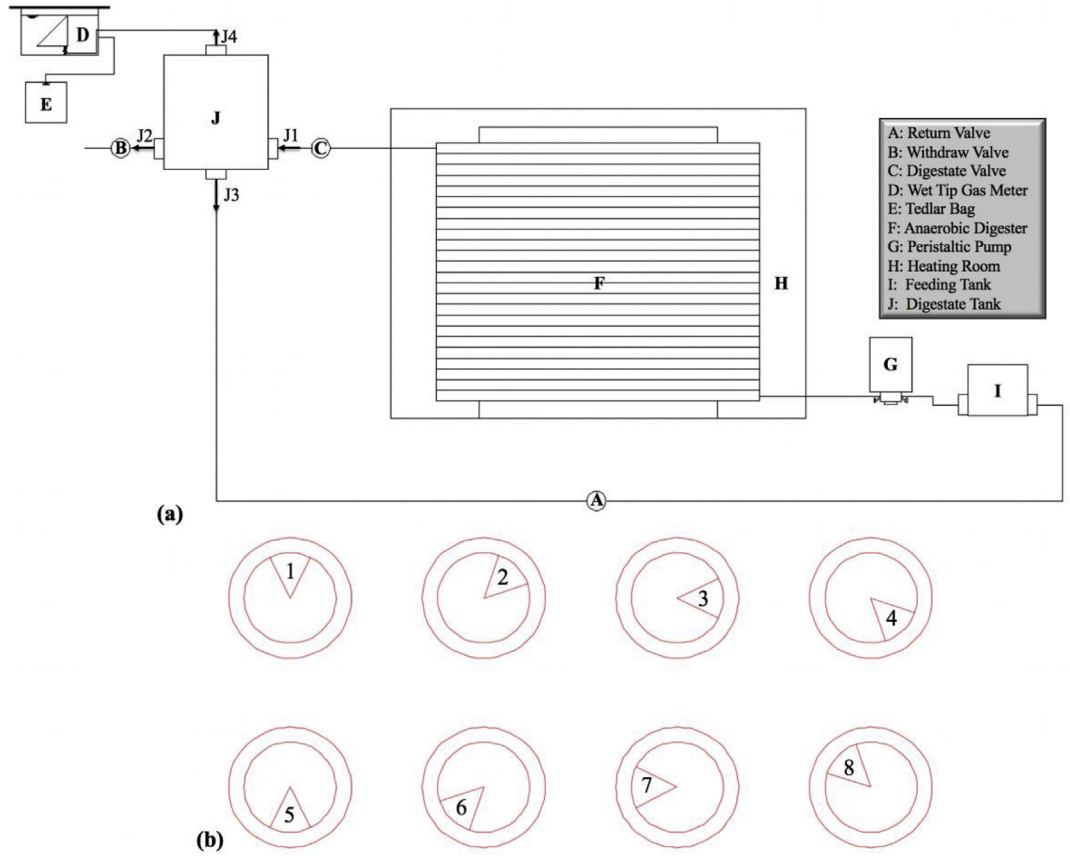

Fig. 1. Experimental setup: (a) side view of the equipment layout; (b) section view of the tubing showing the sequence of pillars as attached to the inner wall in sets of eight.

recommended ranges (1000–2000 mg L^{-1} [35]). Removal efficiencies of solids and COD were determined as the difference between influent and effluent concentrations divided by influent concentration. The pH was monitored, three to five times a week, using a pH probe (Hack, 35641-51).

Biogas samples were collected on a daily basis and fed to a dual wavelength infrared cell with reference channels (GEM-2000 monitor, Keison Products, UK) for analysis. Specific CH_4 yield, expressed as the volume of CH_4 produced per gram VS fed to the digester, was calculated weekly. Where deemed appropriate, the analysis results are reported as average value ± standard deviation.

2.5. CFD modeling

A section of the FSAD was modeled, to represent one winding (YZ plane in Fig. 3) of the coiled structure, comprising an entire set of 8 conical pillars distributed angularly to enhance mixing by local turning of the flow, across all directions. Considering the low TS content, and being interested in passive fluid mixing, incompressible fluid conditions were assumed.

The fluid-flow can be described at steady-state by solving the Navier-Stokes equations (dimensional):

$$\nabla.\boldsymbol{u} = 0 \tag{1}$$

$$\rho\boldsymbol{u}.\nabla\boldsymbol{u} = -\nabla p + \mu\nabla^2\boldsymbol{u}. \tag{2}$$

where, $\boldsymbol{u} = [u, v, w]^T$ is the fluid velocity (along X, Y, and Z, respectively), p is the fluid pressure, ρ is the fluid density, and μ is the dynamic viscosity. Given the longtime experimental simulation (five and seven HRT for the first and second experimental parts, respectively), steady-state conditions were assumed. After solving for the steady-state fluid flow, the propagation of the constituent wastes was modeled using a (passive) scalar transport equation:

$$\frac{\partial\varphi}{\partial t} + \boldsymbol{u}.\nabla\varphi = \nabla.(D\nabla\varphi) \tag{3}$$

where, φ is the concentration, and D is the diffusion coefficient (taken to be very low for convection-dominated transport). Since this work does not examine transient effects, it solves for background flow-field first and then for the steady-state scalar field for the developed flow. ANSYS Fluent 18.1 was used to solve these equations on an unstructured mesh using a Finite-Volume method. A uniform inlet velocity and a zero-pressure outlet condition were used, along with no-flux conditions for the concentration on all boundaries except the inlet, where a fixed value is prescribed.

3. Results and discussions

3.1. System performance

3.1.1. Stability

During start-up (weeks 1–5), the pH level was slightly below neutral (6.61 ± 0.21), which required the addition of an alkaline solution (20 mL of NaOH 5M) during feeding. Afterward, the pH stabilized at 6.95 ± 0.24 (Fig. 4-a) – considered satisfactory [5]. During steady-state operation of the AnPFR (weeks 6–16), the average VFA concentration was 4433 ± 777 mg L^{-1}, higher than the recommended concentration for stable performance (1000–2000 mg L^{-1} [35] (Fig. 4-a). Ammonia concentration was

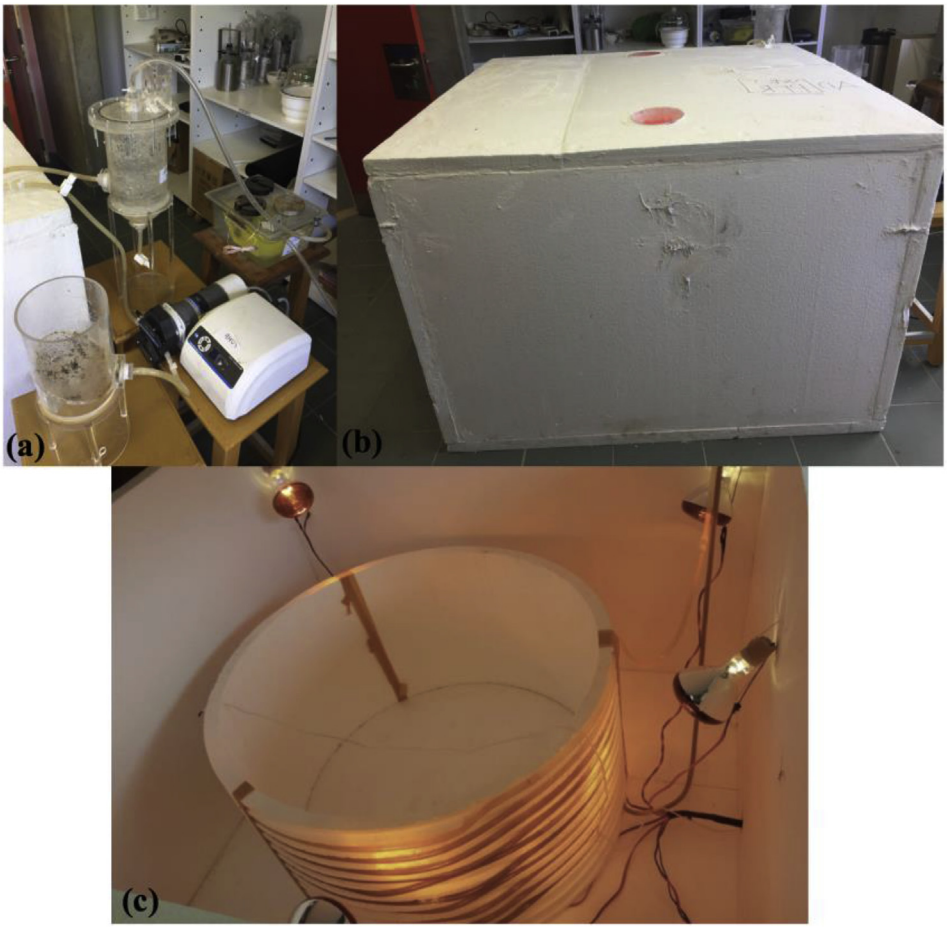

Fig. 2. Experimental Setup: (a) Feeding tank, peristaltic tank, and digestate tank; (b) constant temperature chamber; (c) FSAD tube, coiled around a Styrofoam cylinder.

Table 1
Feed characteristics.

Parameters	Feed
% VS	2.1
% TS	2.5
COD (mg.L^{-1})	51,234
VS/TS	0.84
FW-to-WW	1 to 9
Inlet Kinetic Viscosity (m^{2}s^{-1})	2.53*10^{-5}
Outlet Kinetic Viscosity (m^{2}s^{-1})	1.27*10^{-5}

about 547 ± 15 mg L^{-1}, similar to reported values [29,30]. Total alkalinity, considered as the buffering capacity of the digester, started at an average of 3200 ± 943 mg L^{-1} during the start-up and stabilizing at 5465 ± 781 mg L^{-1} during steady-state operation (weeks 6–16). The observed alkalinity falls within reported ranges (4500 and 15,000 mg L^{-1}) for AD of FW [36].

In comparison, upon upgrading the AnPFR into FSAD (by introducing the passive mixing pillars, weeks 17–30), ammonia concentration decreased slightly to 531 ± 16 mg L^{-1}, with a noticeable decrease in both VFA and Alkalinity concentrations, reaching 2033 ± 144 mg L^{-1} and 4126 ± 242 mg L^{-1}, respectively (Fig. 4), and an increase in pH to 7.14 ± 0.07, indicating improved stability of the system [5,35].

3.1.2. Methane generation

During AnPFR operation, the average specific biogas and methane yields were 462 ± 9 L kg VS_{fed}^{-1} and 181 ± 6 L kg VS_{fed}^{-1}, respectively (Fig. 4-b), which is considered low for AD of FW [27]. The low methane yield can be attributed to the settlement of solids at the bottom of the tubing, in the absence of mixing, hence increasing the concentration of acids, and other digestion

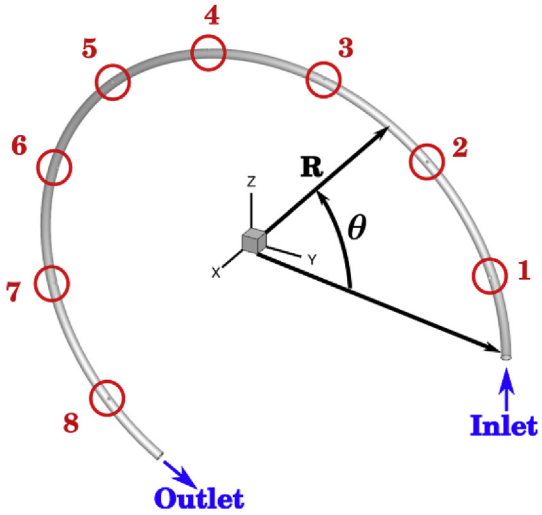

Fig. 3. Computational domain: one winding of the FSAD coil, with a set of 8 conical pillars numbered as shown.

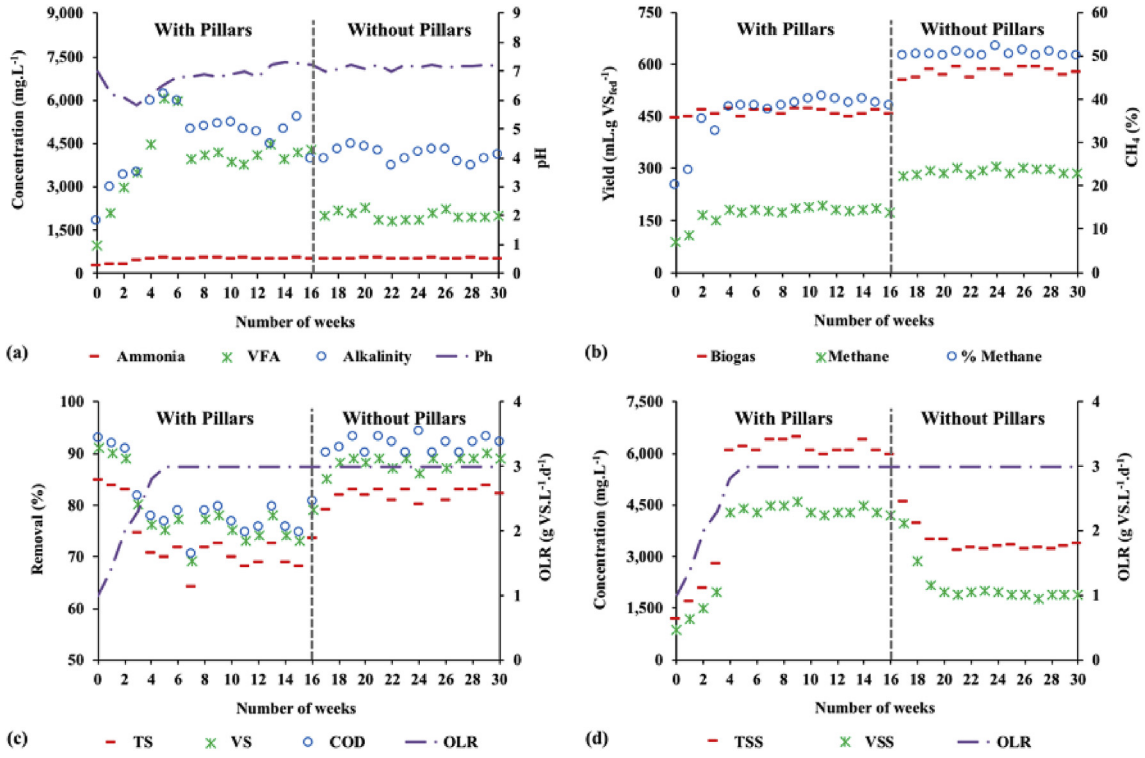

Fig. 4. Performance in terms of: (a) VFA, Alkalinity, and Ammonia Concentrations, (b) CH_4 and Biogas Yields, (c) TS and VS removal, and (d) TSS and VSS concentrations.

byproducts, in high-solid niches. This leads to partial inhibition of methanogenic activities [2,37]. Upon shifting to FSAD operation, by introducing passive mixing through pillars, the methane yield increased by 61% to reach 292 ± 9 L CH_4.kg VS_{fed}^{-1}.

3.1.3. Treatment efficiency

During the AnPFR's operation (weeks 6–16), at OLR of 3.0 g $VS.L^{-1}.d^{-1}$, the removal efficiencies were 70 ± 3%, 75 ± 3%, and 77 ± 3% for TS, VS, and COD, respectively (Fig. 4-c). Upon shifting to FSAD (weeks 17–30), the treatment efficiency of the system was substantially enhanced, and the removal efficiencies reached 82% ± 2% for TS, 88% ± 2% for VS, and 91 ± 2% for COD (Fig. 4-c). Similar removal efficiencies were reported for mesophilic AD of FW, ranging between 82% and 91% for COD and 72% and 92% for VS, at an OLR ranging from 1.5 to 3.5 g $VS.L^{-1}.d^{-1}$ [38–42]. The VSS, which is often considered an indication of microbial abundance, represented 70 ± 1% of the TSS and was fairly stable throughout the experiment: 4367 ± 130 mg L^{-1} between weeks 6 and 16, and 2184 ± 153 mg L^{-1} between weeks 17 and 30 (Fig. 4-d).

3.2. CFD model outputs

3.2.1. Mesh convergence

Since the effective Reynolds number in this system is low (~14), no turbulence model needs to be considered. Therefore, mesh convergence analysis was first performed on increasingly refined meshes. Four sizes of meshes (0.5, 1, 2, and 4 million nodes) were compared. The vorticity magnitude at the channel centerline and average wall-shear across the channel walls were observed. From Fig. 5a, it was found that the flow-fields converge for higher

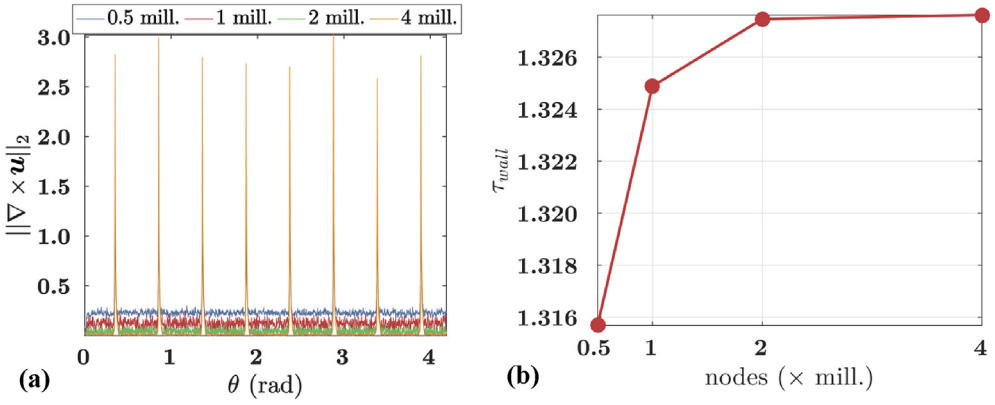

Fig. 5. Mesh convergence: (a) vorticity-magnitude at the channel centerline as a function of the angle (inlet to outlet) for different refinements (b) average wall-shear for different refinement.

Table 2
Flow-field: volumetric integrals of normalized absolute value of u-component of velocity and vorticity magnitude.

Volumetric Integrand	Without pillars	With pillars
$\|\boldsymbol{u}\|$	0.188	0.717
$\frac{\|\|\nabla \times \boldsymbol{u}\|\|_2}{\left(\frac{U}{D}\right)}$	378.42	392.81

refinements (2 and 4 million nodes), with vorticity peaks at the pillar locations and minimal fluctuations far from pillars. Also, from Fig. 5b, the average wall-shear shows negligible change after two million nodes, which shows convergence in the wall refinements. Hence, the two-million nodes was picked as a converged refinement for further cases involving scalar transport.

3.2.2. Impact of pillars

Flow quantities, such as volume-integrated absolute u velocity and vorticity magnitude, were observed (Table 2). The integrated radial velocity components for the unobstructed and obstructed cases are 48.87, and 50.22, respectively. Similarly, the angular components measure 248.87, and 251.13, respectively.

It is observed that while all the quantities are higher when pillars obstruct the flow, the u velocity component is significantly higher than the unobstructed case. The vorticity, and velocity magnitude fields, and streamlines are shown in Fig. 6 to examine the effect of pillars on the flow. As mentioned before, the pillars produce a sharp peak in local vorticity of the flow, thereby giving a turning effect to the fluid, and this is also evident from Fig. 6 This effect can be expected to compound due to finite inertia of the fluid and the spatial arrangement of the pillars. The finite vorticity components in the plane of the coil act to enhance mixing. It is also seen that the vorticity distribution and the sign of vorticity at each pillar vary as a function of the pillar location and orientation, and this non-uniformity may be essential for the overall gain in efficiency in terms of mixing. In this respect, the advection-maps (Fig. 7) were calculated, as reported by previous researchers in the context of flow-sculpting [23]. These maps essentially map the migration of cross-sectional "cells" or parcels of fluid (and hence the solid matter) from their initial locations (before the pillar) to new locations (after the pillar). The transition maps for the current case reveal that fluid (and solid matter) near pillars is spread out from the pillars downstream, and fluid away from the pillars and close to the walls is drawn closer to the center.

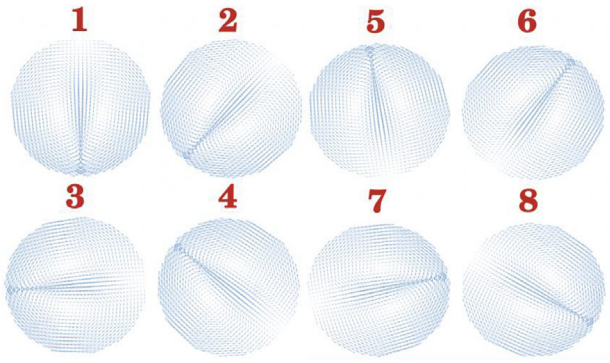

Fig. 7. Flow-field: advection maps (quivers) across pillars (numbered) - length of quivers indicates larger displacements and direction indicates direction of migration.

Next, the study examines the concentration of a scalar of low diffusivity (which mimics solid parcel moving in flow) released in a fully-developed flow. The inlet boundary condition is given by the coordinates: $0.249 \leq R\ (in\ m) \leq 0.251$, $-0.0047 \leq X\ (in\ m) \leq 0.0047$. Fig. 8 shows the concentrations at cross-sectional slices before, at, and after the first pillar. It is seen from the scalar field that the pillar creates a spread in the concentration which enhances mixing. In contrast, it is evident that the concentration is uniform in the angular direction for the traditional designs (no pillars). However, for the FSAD, local mixing of the transported scalar (wastes) is fortified by the clockwise-pattern arrangement of the 8 pillars, which serve to successively induce inertia and deformation in out-of-plane directions. The *Dean number (De)* for the present case is calculated to be ≈ 1, and gives a relative estimate of the competing inertial, centripetal, and viscous forces. It is also worth noting that the curvature of the pipe also

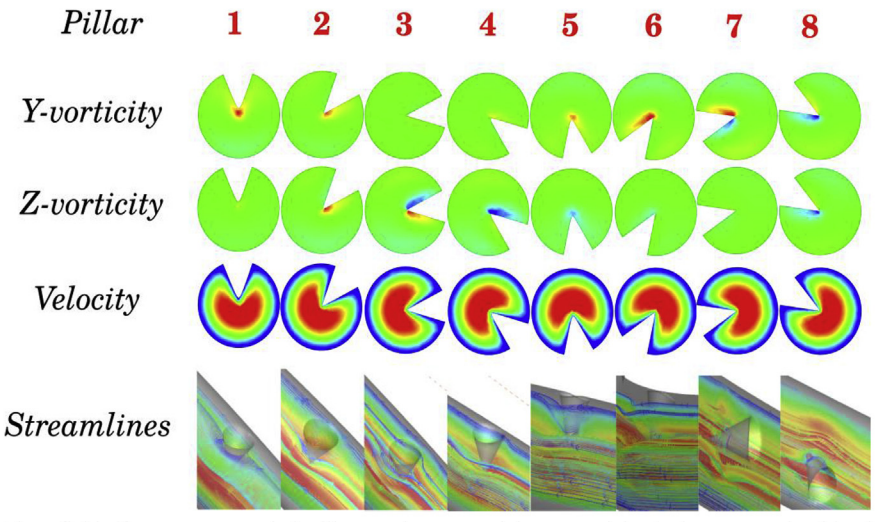

Fig. 6. Flow-field: (from top, row-wise) pillar number, y-vorticity, z-vorticity (color map: red to blue indicate positive to negative values), velocity-magnitude, and streamlines around the pillars (colored by velocity-magnitude). (For interpretation of the references to color in this figure legend, the reader is referred to the Web version of this article.)

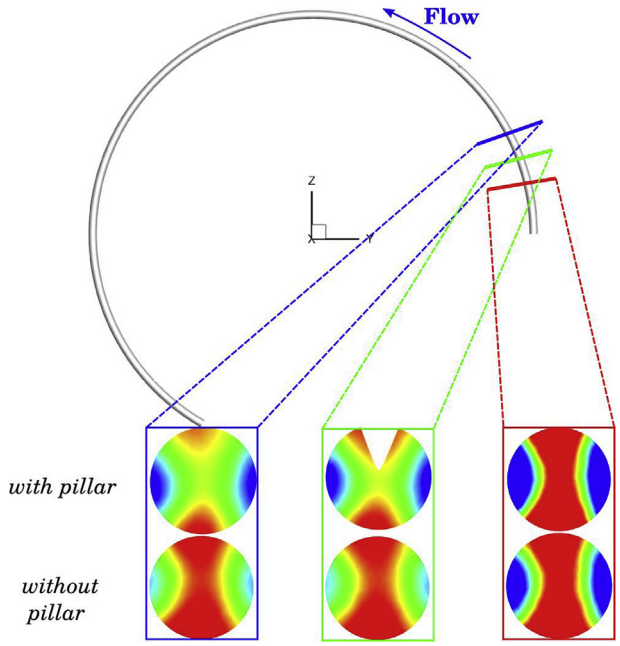

Fig. 8. Evolution of scalar field across pillar-1: in the absence of pillars (traditional AnPFR) and in the presence of pillars (FSAD). The green section marks the location of pillar-1, the red and blue sections mark locations upstream and downstream of pillar-1, respectively; contour values are equalized within each cross-section for pillar-1. (For interpretation of the references to color in this figure legend, the reader is referred to the Web version of this article.)

plays a role in creating a slightly asymmetric concentration field, which is attributed to low De.

3.3. Benefits of FSAD

The studied system was stable even during the period of no mixing (weeks 6–16), which indicates that solids settlement was not detrimental to the process. On the contrary, it can be assumed that syntrophic reactions were enhanced by avoiding the separation of syntrophic microorganisms (e.g. hydrogenotrophic methanogens and hydrogen generating bacteria) by mixing [3]. Yet, in many instances, AnPFRs require physical (radial) mixing to avoid the drawbacks experienced in stagnant designs, including, but not limited to: (1) dead zones, (2) local accumulation of inhibiting by-products, (3) uneven distribution of heat, and (4) reduced contact between the nutrients and the microflora [5,43–45]. Accordingly, it was hypothesized that the novel FSAD design would improve the effluent quality and energy generation potential. In fact, the slow mixing during feeding proved to enhance the quality of the effluent by additionally reducing the concentrations of COD, TS, VS, and VFA by 14.8%, 12%, 12.9%, and 54.1%, respectively (Table 3). Equally important, methane generation increased by 61.3%. The observed benefits of the FSAD could be attributed to better accessibility of the nutrient due to enhanced contact with the microorganisms and reduced short-circuiting. Yet, this phenomenon can have a positive effect only if the digestion byproducts remain below inhibitory levels, which is more likely to occur in the presence of mixing due to mechanical dispersion. Furthermore, by visual inspection, the induced mixing (by up-flow pumping of 11 mL s^{-1}) seems slow, which is expected to reduce potential disturbance of syntrophic interactions – yet this observation requires further investigation.

4. Conclusions

This study investigates the performance of a novel anaerobic PFR design for the treatment of a mixture of FW and WW, at an OLR of 3 g $VS.L^{-1}.d^{-1}$, and a low TS content of 2.5%. The novel design introduces passive mixing by flow sculpting via a series of obstructions (pillars) inserted throughout the length of the digester, and was therefore called Flow Sculpting enabled Anaerobic Digester (FSAD). The CFD modeling of the system showed that mixing is enhanced in the presence of pillars due to local vorticity created in the fluid in the vicinity of pillars, and an out-of-coil-plane velocity component which is significantly higher than the traditional design. In fact, experimentally, the FSAD design boosted the system efficiency, resulting in a decrease in the VFA concentration by 54%, and an increase of the VS removal, COD removal, and CH_4 yield by 17%, 19%, and 62%, respectively.

Declaration of competing interest

The authors declare that they have no known competing financial interests or personal relationships that could have appeared to influence the work reported in this paper.

CRediT authorship contribution statement

Sophia Ghanimeh: Conceptualization, Methodology, Writing - review & editing, Funding acquisition, Supervision, Project administration. **Charbel Abou Khalil:** Methodology, Investigation, Data curation, Writing - original draft. **Daniel Stoecklein:** Formal analysis, Writing - original draft. **Aditya Kommasojula:** Formal analysis, Writing - original draft. **Baskar Ganapathysubramanian:** Methodology, Writing - review & editing, Funding acquisition.

Table 3
Variation of the FSAD performance before and after mixing.

Parameter	Avg. Value (Without Mixing)	Avg. Value (With Mixing)
pH	6.95	7.14
VS ($mg.L^{-1}$)	5214	2503
TS ($mg.L^{-1}$)	7523	4523
COD ($mg.L^{-1}$)	11,938	4334
VSS ($mg.L^{-1}$)	4367	2184
TSS ($mg.L^{-1}$)	6200	3463
Biogas Yield ($L.kg\ VS^{-1}$)	462	577.5
CH_4 Yield ($L.kg\ VS^{-1}$)	180.8	291.6
VFA ($mg.L^{-1}$)	4433	2034
Alkalinity ($mg.L^{-1}$)	5465	4127
Ammonia ($mg.L^{-1}$)	546.7	530.8

Acknowledgment

This research was funded by the National Council for Scientific Research, Lebanon (CNRS-L), under the Grant Research Program (GRP). Also, this work was partially supported by The National Academies of Sciences, Engineering and Medicine, Washington, DC, through the Arab-American Frontiers Fellowship Fund.

References

[1] S. Sakar, K. Yetilmezsoy, E. Kocak, Anaerobic digestion technology in poultry and livestock waste treatment—a literature review, Waste Manag. Res. 27 (2009) 3–18, https://doi.org/10.1177/0734242X07079060.
[2] L. Appels, J. Lauwers, J. Degrève, L. Helsen, B. Lievens, K. Willems, R. Dewil, Anaerobic digestion in global bio-energy production: potential and research challenges, Renew. Sustain. Energy Rev. 15 (9) (2011) 4295–4301, https://doi.org/10.1016/j.rser.2011.07.121.
[3] T. Amani, M. Nosrati, S.M. Mousavi, R.K. Kermanshahi, Study of syntrophic anaerobic digestion of volatile fatty acids using enriched cultures at mesophilic conditions, Int. J. Environ. Sci. Te. 8 (2011) 83–96, https://doi.org/10.1007/BF03326198.
[4] N.D. Manser, J.R. Mihelcic, S.J. Ergas, Semi-continuous mesophilic anaerobic digester performance under variations in solids retention time and feeding frequency, Bioresour. Technol. 190 (2015) 359–366, https://doi.org/10.1016/j.biortech.2015.04.111.
[5] C. Mao, Y. Feng, X. Wang, G. Ren, Review on research achievements of biogas from anaerobic digestion, Renew. Sustain. Energy Rev. 45 (2015) 540–555, https://doi.org/10.1016/j.rser.2015.02.032.
[6] M. Sattler, Favoring Anaerobic Wastewater Treatment: A Call for a Paradigm Shift, Annual Conference and Exhibition, Air and Waste Management Association, 2011.
[7] A. Pfluger, J. Coontz, V. Zhiteneva, T. Gulliver, L. Cherry, L. Cavanaugh, L. Figueroa, Anaerobic digestion and biogas beneficial use at municipal wastewater treatment facilities in Colorado: a case study examining barriers to widespread implementation, J. Clean. Prod. 206 (2019) 97–107, https://doi.org/10.1016/j.jclepro.2018.09.161.
[8] F. Di Maria, M. Barratta, Boosting methane generation by co-digestion of sludge with fruit and vegetable waste: internal environment of digester and methanogenic pathway, Waste Manag. 43 (2015) 130–136, https://doi.org/10.1016/j.wasman.2015.06.007.
[9] G. Lettinga, Anaerobic digestion and wastewater treatment systems, Antonie Leeuwenhoek 67 (1995) 3–28, https://doi.org/10.1007/BF00872193.
[10] B. Ma, Y. Peng, S. Zhang, J. Wang, Y. Gan, J. Chang, G. Zhu, Performance of anammox UASB reactor treating low strength wastewater under moderate and low temperatures, Bioresour. Technol. 129 (2013) 606–611, https://doi.org/10.1016/j.biortech.2012.11.025.
[11] L.B. Chu, F.L. Yang, X.W. Zhang, Anaerobic treatment of domestic wastewater in a membrane-coupled expended granular sludge bed (EGSB) reactor under moderate to low temperature, Process Biochem. 40 (2005) 1063–1070, https://doi.org/10.1016/j.procbio.2004.03.010.
[12] B. Lew, S. Tarre, M. Beliavski, C. Dosoretz, M. Green, Anaerobic membrane bioreactor (AnMBR) for domestic wastewater treatment, Desalination 243 (2009) 251–257, https://doi.org/10.1016/j.desal.2008.04.027.
[13] S. Chang, Anaerobic membrane bioreactors (AnMBR) for wastewater treatment, Adv. Mater. Res-Switz 4 (2014) 56–61, https://doi.org/10.4236/aces.2014.41008.
[14] L. Seghezzo, G. Zeeman, J.B. van Lier, H.V.M. Hamelers, G. Lettinga, A review: the anaerobic treatment of sewage in UASB and EGSB reactors, Bioresour. Technol. 65 (1998) 175–190, https://doi.org/10.1016/S0960-8524(98)00046-7.
[15] A. Torkian, A. Eqbali, S.J. Hashemian, The effect of organic loading rate on the performance of UASB reactor treating slaughterhouse effluent, Resour. Conserv. Recycl. 40 (2003) 1–11, https://doi.org/10.1016/S0921-3449(03)00021-1.
[16] J.P. Guyot, H. Macarie, A. Noyola, Anaerobic digestion of a petrochemical wastewater using the UASB process, Appl. Biochem. Biotechnol. 24 (1990) 579–589.
[17] J. Ho, S. Sung, Methanogenic activities in anaerobic membrane bioreactors (AnMBR) treating synthetic municipal wastewater, Bioresour. Technol. 101 (2010) 2191–2196, https://doi.org/10.1016/j.biortech.2009.11.042.
[18] S. Lansing, J.F. Martin, R.B. Botero, T.N. Da Silva, E.D. Da Silva Ed, Methane production in low-cost, unheated, plug-flow digesters treating swine manure and used cooking grease, Bioresour. Technol. 101 (2010) 4362–4370.
[19] V.K. Sharma, C. Testa, G. Lastella, G. Cornacchia, M.P. Comparato, Inclined-plug-flow type reactor for anaerobic digestion of semi-solid waste, Appl. Energy 65 (2000) 173–185, https://doi.org/10.1016/S0306-2619(99)00084-7.
[20] P. Namsree, W. Suvajittanont, C. Puttanlek, D. Uttapap, V. Rungsardthong, Anaerobic digestion of pineapple pulp and peel in a plug-flow reactor, J. Environ. Manag. 110 (2012) 40–47, https://doi.org/10.1016/j.jenvman.2012.05.017.
[21] C.H. Burnett, A.P. Togna, New high-rate plug flow anaerobic digester technology for small communities, in: Proceeding of the IWA Conference on Biosolids, Moving Forward Wastewater Biosolids Sustainability: Technical, Managerial, and Public Synergy, 2007, pp. 24–27.
[22] D. Stoecklein, K.G. Lore, M. Davies, S. Sarkar, B. Ganapathysubramanian, Deep learning for flow sculpting: insights into efficient learning using scientific simulation data, Sci. Rep-UK 7 (2017) 46368, https://doi.org/10.1038/srep46368.
[23] D. Stoecklein, C.Y. Wu, D. Kim, D. Di Carlo, B. Ganapathysubramanian, Optimization of micropillar sequences for fluid flow sculpting, Phys. Fluids 28 (2016), 012003, https://doi.org/10.1063/1.4939512.
[24] S.H. Kim, S.K. Han, S.H. Shin, Two-phase anaerobic treatment system for fat-containing wastewater, J. Chem. Technol. Biotechnol. 79 (2004) 63–71, https://doi.org/10.1016/j.ijhydene.2004.02.018.
[25] P. Sosnowski, A. Wieczorek, S. Ledakowicz, Anaerobic co-digestion of sewage sludge and organic fraction of municipal solid wastes, Adv. Environ. Res. 7 (2003) 609–616, https://doi.org/10.1016/S1093-0191(02)00049-7.
[26] K. Latha, R. Velraj, P. Shanmugam, S. Sivanesan, Mixing strategies of high solids anaerobic co-digestion using food waste with sewage sludge for enhanced biogas production, J. Clean. Prod. 210 (2009) 388–400, https://doi.org/10.1016/j.jclepro.2018.10.219.
[27] EPA, in: Anaerobic Digestion of Food Waste, FINAL REPORT, East Bay Municipal Utility District (EBMUD), 2008. https://archive.epa.gov/region9/organics/web/pdf/ebmudfinalreport.pdf. (Accessed 21 September 2014).
[28] H.M. Jang, J.H. Ha, J.M. Park, M.S. Kim, S.G. Sommer, Comprehensive microbial analysis of combined mesophilic anaerobic–thermophilic aerobic process treating high-strength food wastewater, Water Res. 73 (2015) 291–303, https://doi.org/10.1016/j.watres.2015.01.038.
[29] S. Ghanimeh, C.A. Khalil, C.B. Mosleh, C. Habchi, Optimized anaerobic-aerobic sequential system for the treatment of food waste and wastewater, Waste Manag. 71 (2018a) 767–774.
[30] S. Ghanimeh, C. Abou Khalil, E. Ibrahim, Anaerobic digestion of food waste with aerobic post-treatment: effect of fruit and vegetable content, Waste Manag. Res. 36 (2018) 965–974.
[31] L. Xin, Z. Guo, X. Xiao, W. Xu, R. Geng, W. Wang, Feasibility of anaerobic digestion for contaminated rice straw inoculated with waste activated sludge, Bioresour. Technol. 266 (2018) 45–60, https://doi.org/10.1016/j.biortech.2018.06.048.
[32] G. Lastella, C. Testa, G. Cornacchia, M. Notornicola, F. Voltasio, V.K. Sharma, Anaerobic digestion of semi-solid organic waste: biogas production and its purification, Energy Convers. Manag. 43 (2002) 63–75, https://doi.org/10.1016/S0196-8904(01)00011-5.
[33] APHA (American Public Health Association), AWWA (American Water Works and Protection Association) and WPCF (Water Pollution Control Federation), twentyth ed., Standard Methods for the Examination of Water and Wastewater, Washington, DC, 2012.
[34] L.E. Ripley, W.C. Boyle, J.C. Converse, Improved alkalimetric monitoring for anaerobic digestion of high-strength wastes, Water Pollut. Control (1986) 406–411. https://www.jstor.org/stable/25042933.
[35] S. Jayalakshmi, K. Joseph, V. Sukumaran, Bio hydrogen generation from kitchen waste in an inclined plug flow reactor, Int. J. Hydrogen Energy 34 (2009) 8854–8858, https://doi.org/10.1016/j.ijhydene.2009.08.048.
[36] H.O. Méndez-Acosta, B. Palacios-Ruiz, V. Alcaraz-González, J.P. Steyer, V. González-Álvarez, E. Latrille, Robust control of volatile fatty acids in anaerobic digestion processes, Ind. Eng. Chem. Res. 47 (2008) 7715–7720, https://doi.org/10.1021/ie800256e.
[37] K. Karim, K.T. Klasson, R. Hoffmann, S.R. Drescher, D.W. DePaoli, M.H. Al-Dahhan, Anaerobic digestion of animal waste: effect of mixing, Bioresour. Technol. 91 (2005) 1607–1612, https://doi.org/10.1016/j.biortech.2004.12.021.
[38] R. Ganesh, M. Torrijos, P. Sousbie, A. Lugardon, J.P. Steyer, J.P. Delgenes, Single-phase and two-phase anaerobic digestion of fruit and vegetable waste: comparison of start-up, reactor stability and process performance, Waste Manag. 34 (2014) 875–885, https://doi.org/10.1016/j.wasman.2014.02.023.
[39] J. Kim, J.T. Novak, Combined anaerobic/aerobic digestion: effect of aerobic retention time on nitrogen and solids removal, Water Environ. Res. 83 (2011) 802–806, https://doi.org/10.2175/106143011X12928814444970.
[40] D.H. Kim, S.E. Oh, Continuous high-solids anaerobic co-digestion of organic solid wastes under mesophilic conditions, Waste Manag. 31 (2011) 1943–1948, https://doi.org/10.1016/j.wasman.2011.05.007.
[41] A. Serrano, J.A. Siles, A.F. Chica, M.A. Martin, Improvement of mesophilic anaerobic co-digestion of agri-food waste by addition of glycerol, J. Environ. Manag. 140 (2014) 76–82, https://doi.org/10.1016/j.jenvman.2014.02.028.
[42] L. Wang, F. Shen, H. Yuan, D. Zou, Y. Liu, B. Zhu, X. Li, Anaerobic co-digestion of kitchen waste and fruit/vegetable waste: lab-scale and pilot-scale studies, Waste Manag. 34 (2014) 2627–2633, https://doi.org/10.1016/j.wasman.2014.08.005.
[43] S. Ghanimeh, M. El-Fadel, P. Saikaly, Improving the stability of thermophilic anaerobic digesters treating SS-OFMSW through enrichment with compost and leachate seeds, Bioresour. Technol. 131 (2013) 53–59, https://doi.org/10.1016/j.biortech.2012.12.127.
[44] X. Gomez, M.J. Cuetos, J. Cara, A. Moran, A.I. Garcia, Anaerobic co-digestion of primary sludge and the fruit and vegetable fraction of the municipal solid wastes: conditions for mixing and evaluation of the organic loading rate, Renew. Energy 31 (12) (2006) 2017–2024, https://doi.org/10.1016/j.renene.2005.09.029.
[45] F. Conti, L. Wiedemann, M. Sonnleitner, A. Saidi, Monitoring the mixing of an artificial model substrate in a scale-down laboratory digester, Renew. Energy 132 (2019) 351–362, https://doi.org/10.1016/j.renene.2018.08.013.